Experimental Characterization of Unsteady Wake Dynamics using Instationary Pressure-Sensitive Paint

By M. Bitter, T. Hara†, D. Yorita†, K. Asai† AND C. J. Kähler
Institut für Strömungsmechanik und Aerodynamik, Universität der Bundeswehr München
Werner-Heisenberg-Weg 39, 85577 Neubiberg

This report summarizes the results of time-resolved pressure-sensitive paint measurements conducted within the first *SFB/TRR 40 Summer Program* at the base and sting of a generic space launcher configuration. In this collaborative work, the unsteady pressure fluctuations were examined by conventional (*kulite*) and optical (instationary pressure-sensitive paint, iPSP) measurement techniques.

The iPSP measurement technique worked well and revealed its potential in the trisonic wind tunnel facility up to sampling-rates of 4 kHz. The first results of the power spectra density showed a good correlation between *kulite* pressure transducer signals and iPSP. A first analysis of the pressure fluctuations in the base area confirmed the assumption of the presence of circumferentially distributed mode-like structures which were predicted by numerical simulations.

1. Introduction

In order to characterize the dynamics of coherent vorticial structures developing in the wake area of the generic space transportation system, detailed time-resolved velocity field measurements were recently performed, see [1]. For a quantitative evaluation of these structures with respect to the main scientific questions: *1. How is the dynamic and strength of the coherent wake structures? 2. Are these dynamics characterized by a certain frequency? 3. Does the boundary layer- wake interaction result in a coherent mode pattern on the base? 4. Is this mode pattern somehow time-dependent?*, instationary pressure-sensitive paint (iPSP) measurements were performed within the first *SFB/TRR 40 Summer Program* at the Institute of Fluid Mechanics and Aerodynamics of the Bundeswehr University Munich (*UniBwM*). The pressure-sensitive paint measurement technique is an optical measurement technique where the fluorescence intensity of an excited oxygen-sensitive molecule is measured using a photodetector (CCD, CMOS, PMT, $\cdots$), compare [2]. The molecules are typically embedded in a binder material and sprayed on model surfaces for aerodynamic testing. The physical principle is the photochemically deactivation of excited molecules by the oxygen-quenching process. The oxygen concentration in air usually correlates with the static pressure. Hence a measurement of oxygen concentration can be converted into a pressure measurement by calibration. Further details on the principle of this measurement technique can be found in [2].

† School of Engineering, Department of Aerospace Engineering, Tohoku University, 6-6-01 Aramaki-Aza-Aoba Aobaku, Sendai 980-8579, Japan

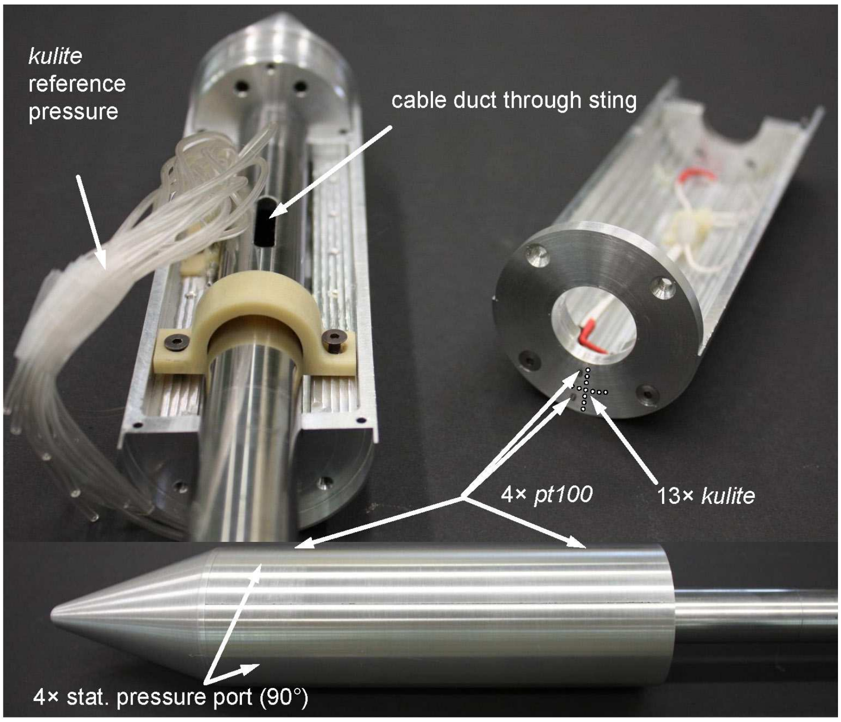

FIGURE 1. Modular iPSP model made from aluminum. The model is equipped with 13 unsteady pressure transducers (*kulite*) steady pressure ports and *pt100* temperature sensors. During the tests, the mounted model in the test section performed a spiral motion with $f_r = 39.2$ Hz and an amplitude of ± 1 mm.

Preparatory work

Steady pressure-sensitive paint (PSP) measurements were performed in the trisonic wind tunnel (*TWM*) in the institute of Fluid Mechanics and Aerodynamics labs in order to prepare the unsteady pressure-sensitive paint (iPSP) experiments, [3]. The wind tunnel and its infrastructure were presented in [1, 3]. The steady PSP measurements were performed on a *NACA 0012* airfoil, [3]. In order to get experiences in this wind tunnel facility, regarding important parameters on PSP measurements the tests were carried out in terms of preparation of the experimental setup (optical aberrations, distortions), data synchronization and acquisition, paint aging and contamination, and temperature homogenization of the flow, as well as the corresponding model surface. This list of major parameter must be handled carefully for an accurate estimation of surface pressure distributions using luminescent coatings. The tests were carried out at similar flow parameters, which are of major interest in the *TRR 40* subproject at *UniBwM*. The results showed an accurate performance of the steady PSP system, which gave the motivation to perform iPSP measurements. In order to acquire promising time-resolved pressure data, the support of Professor *Keisuke Asai*'s group was necessary. As one of the leading experts in the development and application of steady and instationary pressure-sensitive paints, see [4–6], this partner perfectly matches the requirements for the most promising experimental results. For the instationary pressure measurements, a completely new model, see Fig. 1, was developed and manufactured with respect to the earlier performed velocity field measurements, [1]. The model is equipped with 13

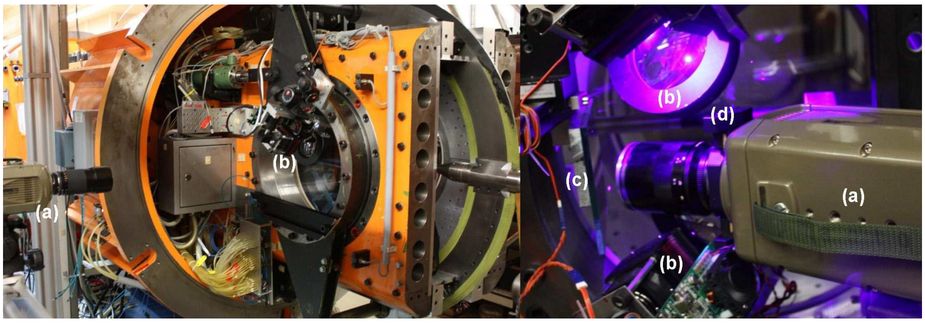

FIGURE 2. Setup at the test section of the trisonic wind tunnel in Munich. Left: port side setup for sting experiments with *Phantom V.12* high-speed *CMOS*-camera (a) and LED illumination (b). Right: starboard setup for base measurements with camera (a), illumination (b), mirror (c) and *Scheimpflug*-angle correction devise (d).

unsteady pressure transducers positioned on the base. The cross-like location of the pressure transducers was chosen in order to measure the pressure fluctuations radially and circumferentially. Markers for image segmentation and correction of model motion were positioned on the surface of the model via *CNC* lathe, hence the precise position of the markers is known.

2. Experimental setup

With respect to the scientific key-questions (Sec. 1) the experiments were split into two campaigns of separated regions of interest (first: iPSP on the sting; second: iPSP on the base). The experimental setup that was used for the corresponding region of interest is shown in Fig. 2. On the left-hand side, the setup for the sting experiments is shown. In both cases a *Phantom V.12* high-speed *CMOS*-camera (a) with 1 MPx resolution and a maximum frame-rate of 6242 frames per second at full resolution was used. For the sting measurements, the camera was positioned outside of the plenum chamber at a distance of d = 1.4 m away from the center line of the body. A 180mm *Zeiss* objective lens was mounted in front of the camera. For the base measurements, the camera was mounted inside the test section. In order to adjust the sharpness of the intensity images in the entire region of interest, a device for *Scheimpflug*-angle correction was used (d). Here, a 100 mm *Zeiss* macro objective lens was used. For iPSP illumination, two *Luminus CBT-120 UV* high power LEDs (b), each with 10W optical power and a 400 nm low pass color filter, were used in both measurement campaigns. For separating the iPSP signal from the excitation signal, a 570 nm long pass filter with transmission $T > 90\,\%$ in the passing band and optical density $OD > 6$ in the blocking band was used. A simultaneous measurement of both regions of interest was not carried out in order to avoid self-illumination on the model due to the reflected luminescence signal from the paint on adjacent surfaces. For the same reason, the region that was not of interest was covered with an anti-reflection coating. Figure 3 shows the two regions of interest covered with iPSP (magenta) and anti-reflection coating (black). For iPSP a special oxygen-sensor carrier layer is required, which has a highly porous structure for unsteady interaction of the molecules with the pressure fluctuations. In this case, a polymer-ceramic layer was used. The formulation based on titanium dioxide and water was revealed in [4]. A platinum complex (*PtTFPP*) solved in toluene was used as pressure-sensitive dye. Both components were applied to the model surface by spray-gun.

FIGURE 3. Close-up on the model of the generic space launcher made from aluminum and covered with instationary pressure-sensitive paint (iPSP). The model is equipped with unsteady pressure and temperature sensors; left: coating for sting investigations; right: coating for base investigations.

3. Methodology

Due to the blow-down design of the wind tunnel a strong temperature change within the run time is acting on the model. Due to this effect, a series-like image acquisition of *wind-on* and *wind-off* signal images was chosen. The wind tunnel was started and the recording was started after 15-20 seconds to allow for temperature adaption of the model. Within the recording time of the camera (6-20 seconds, depending on the sampling-rate) the wind tunnel was stopped so that the reference *wind-off* signal images were directly recorded as well. A comparable image acquisition procedure was already chosen for the steady PSP investigations, compare [3], and it revealed its potential for economic data acquisition in this wind tunnel facility. The image number varied between 12000 and 44000 images for each test case. Investigations at Mach numbers 0.3 and 0.7, at several sampling-rates $f_{s,PSP} = [500, 1000, 2000, 4000]$ Hz, were carried out for the sting and the base region of interest. The sampling-rate of the *kulite* sensors was kept constant at $f_{s,kul} = 10000$ Hz.

4. Results

The acquired image data revealed high potential for different temporal and spatial data evaluation and processing methods. The results shown in the following figures represent an early status in data analysis. A joint publication of the most promising results with the collaborators from Japan is intended after a revision of the final results is completed.

4.1. *Power density spectra versus Strouhal number*

The four plots in Figs. 4 and 5 show the power density spectrum versus the Strouhal number for Mach number 0.3 (Fig. 4) and Mach number 0.7 (Fig. 5) measured on the sting (corresponding left) and on the base (corresponding right). The signals plotted in black (top in each figure) present the spectrum derived from the *kulite* signals. Therefore, the signal of four radially distributed sensors was averaged. The gray curves (bottom) show the spectrum derived from the averaged iPSP image intensity of a 7-by-7 px^2 area at a certain point on the base or the sting, respectively. The power density spectrum was computed via the *WELCH* algorithm, implemented in *Matlab*. The time signal was subdivided into *FFT* windows of the size $f_{s,FFT}$, (given in the plots - e.g., if the iPSP sampling-rate was $f_{s,PSP} = 1$ kHz, it was $f_{s,FFT} = 512$ Hz). Additionally a 50 % overlap of the *FFT* windows was used to increase the signal-to-noise ratio. The characteristic Strouhal number (non-dimensionalized frequency $\mathrm{St} = f \cdot c/u$; f - frequency;

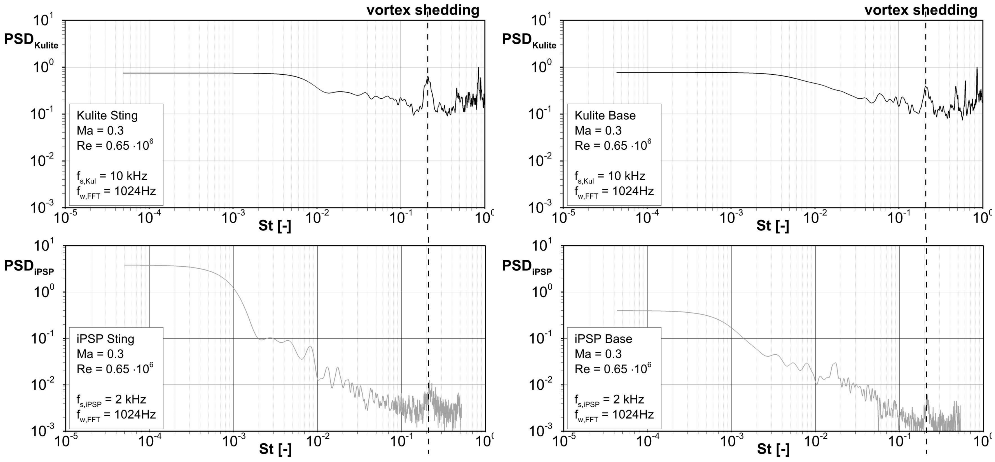

FIGURE 4. Power spectra versus Strouhal number on the sting (left) and on the base (right) measured with *kulites* (top, black) and iPSP (bottom, gray) at Mach number 0.3. The *kulite* sampling-rate was $f_{s,kul} = 10$ kHz and of iPSP it was $f_{s,PSP} = 2$ kHz, respectively. The dashed line indicates the Strouhal number of dominant vortex shedding with Strouhal number $\mathrm{St} = 0.21$ or $f_{shed} \approx 400$ Hz, respectively.

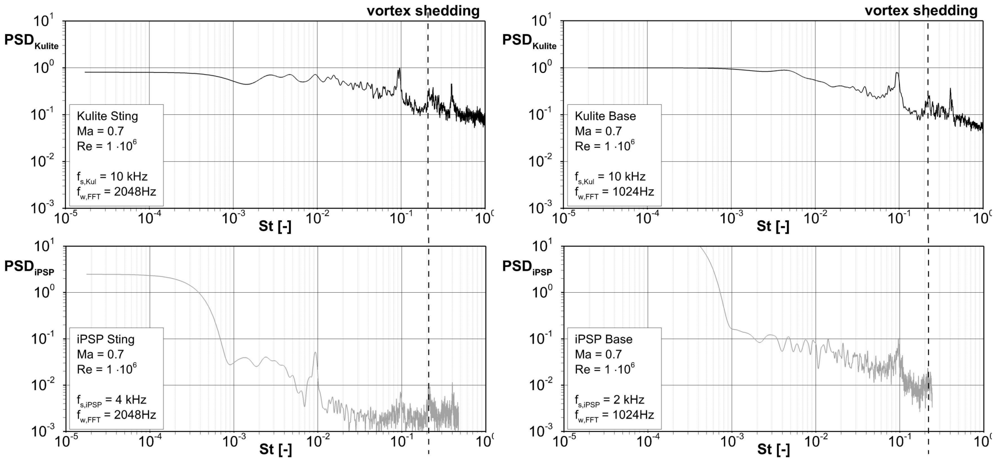

FIGURE 5. Power spectra versus Strouhal number on the sting (left) and on the base (right) measured with *kulites* (top, black) and iPSP (bottom, gray) at Mach number 0.7. The *kulite* sampling-rate was $f_{s,kul} = 10$ kHz and of iPSP it was $f_{s,PSP} = 4$ kHz for the sting experiments and $f_{s,PSP} = 2$ kHz for the base experiments, respectively. The dashed line indicates the Strouhal number of dominant vortex shedding with Strouhal number St = 0.21 or $f_{shed} \approx 905$ Hz, respectively.

c - characteristic length; u - velocity) of vortex shedding for this blunt body is expected in the order of $\mathrm{St} = 0.2$, derived from the *Karman* vortex shedding frequency. At Mach number 0.3 the vortex shedding frequency is $f_{shed} \approx 400$ Hz, which correlates well with the expected Strouhal number $\mathrm{St} = 0.21$, extracted from the *kulite* signals (indicated by the black dashed line). With an iPSP sampling-rate of $f_{s,PSP} = 2$ kHz, the peak in the corresponding power spectrum sufficiently develops at $\mathrm{St} = 0.21$ as well. Analogue

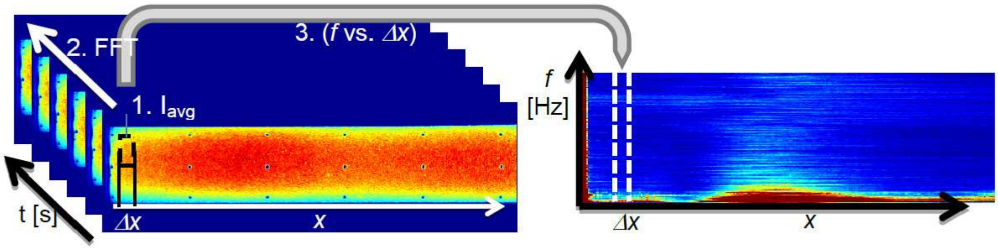

FIGURE 6. Schematic illustrates the signal processing for spatial frequency response evaluation. The analysis is adapted to [7]. First the average intensity (the dashed box) for $\Delta x = 5$ px and $\Delta y = 50$ px is computed. This is done for all images in the time domain, (second step). The signal is converted in the frequency domain by *FFT* and finally plotted with no overlap.

conclusions can be drawn for the base measurements at a Mach number of 0.3 with $f_{s,PSP} = 2$ kHz iPSP sampling-rate.

At Mach number 0.7, compare Fig. 5, the characteristic vortex shedding frequency was $f_{shed} \approx 905$ Hz at $\mathrm{St} = 0.21$. For an adequate time-resolution, an iPSP sampling-rate of $f_{s,PSP} = 4$ kHz was used for the sting measurements. The development of a distinct peak in the corresponding *kulite* and iPSP spectrum can be outlined. For the base measurements, iPSP sampling-rates of only $f_{s,PSP} = 4$ kHz could be used. For a further increase in sampling-rate, the frame-size of the *CMOS* camera had to be cropped significantly. Nevertheless, the development of the characteristic peak at $\mathrm{St} = 0.21$ can also be assumed in this case, see right in Fig. 5.

4.2. *Local frequency spectra*

Figure 6 shows a schematic, which illustrates the signal processing for the sub-sequentially shown local frequency plots. These illustrations, so far, are available for the sting area. At first, the average intensity in a box of $\Delta x = 5$ px and $\Delta y = 50$ px is computed. This is done for all *wind-on* intensity images of the data set. Then the time signal is converted in the frequency response by *FFT* using the same *FFT* window-size as above. The evaluation procedure was derived from [7]. Finally the frequency response is plotted versus the axial sting position x.

In Figs. 7 and 8 the local development of the frequency response along the sting is shown for Mach numbers 0.3 (Fig. 7) and 0.7 (Fig. 8). It can be seen that the characteristic frequency of vortex shedding (compare Sec. 4.1) is dominant along the entire length of the region of interest. In the region where the shedding vortices reattach to the surface of the sting, a broader frequency spectrum, compared to the rest, is visible. This leads to the assumption that the reattachment location varies in position and frequency as well. The dashed line in Fig. 8 at about 250 Hz is an artifact from the computations and is not yet classified. A similar plot for the base area is under preparation at the moment. Therefore, all images must be mapped onto a regular grid and then distorted in the cylindrical plane. This analysis will be included in the final joint publication as well as enhanced spatial evaluation on wavelength and phase shift. However, the results show that the pressure signature of the coherent vortices in the wake can be resolved by the use of the instationary pressure-sensitive paint measurement technique. It could also be confirmed by this technique that a dominant vortex shedding frequency exist.

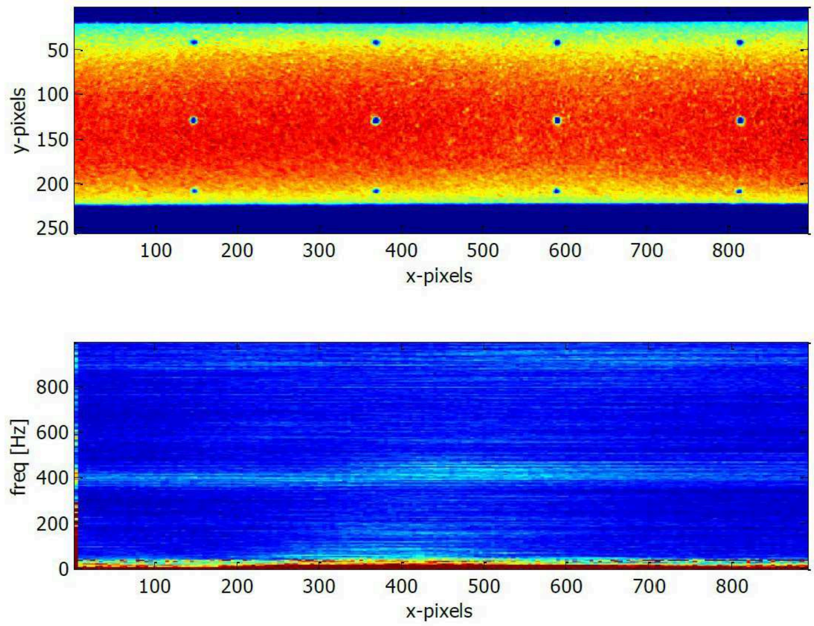

FIGURE 7. Local frequency spectrum along the sting for Mach number 0.3 and iPSP sampling-rate of $f_{s,PSP} = 2\,$kHz.

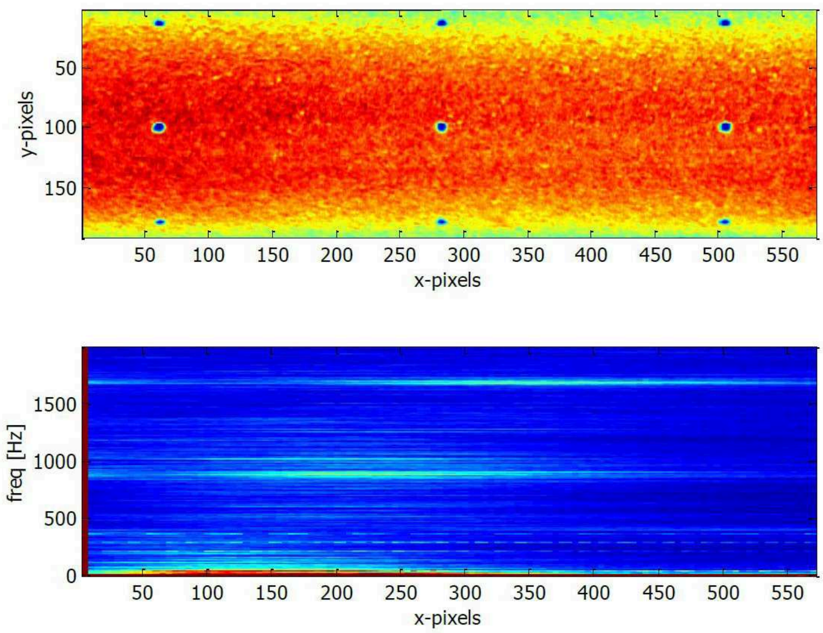

FIGURE 8. Local frequency spectrum along the sting for Mach number 0.7 and iPSP sampling-rate of $f_{s,PSP} = 4\,$kHz.

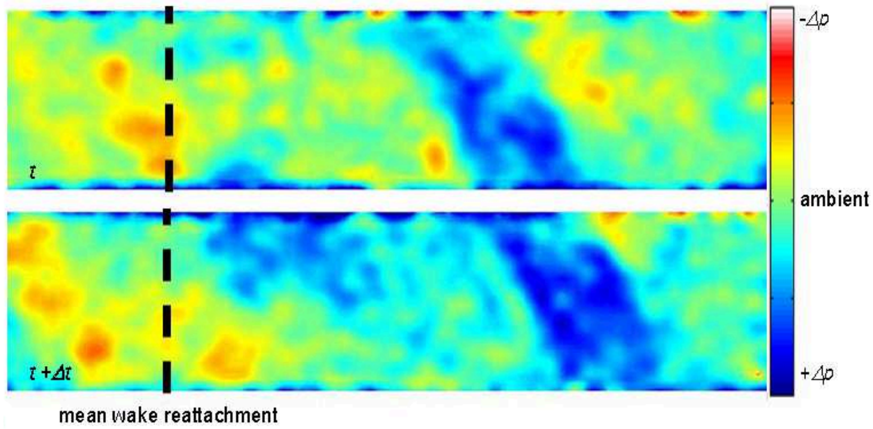

FIGURE 9. Convection of coherent vortex structures on the sting for 2 time steps ($\Delta t = 0.003\,$s) at $\mathrm{Ma} = 0.3$, red indicates low pressure regions and blue high pressure regions, respectively. The dashed line shows the spatial position of the mean wake vortex reattachment.

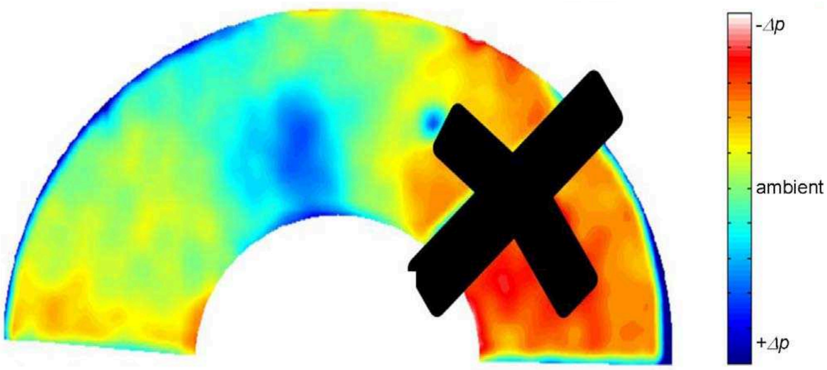

FIGURE 10. Color-coded distribution of pressure modes on the base measured with iPSP at $\mathrm{Ma} = 0.7$. Red indicates low pressure regions and blue high pressure regions, respectively.

4.3. *Visualization of coherent structures*

In Fig. 9 the intensity distributions with equivalent high and low pressure regions are shown for two time steps with $\Delta t = 0.003\,$s measured at Mach number 0.3 with a sampling-rate of $f_{s,PSP} = 1\,$kHz. The dashed line represents the reattachment location of the mean wake recirculation. The convection of a large coherent structure along the sting can be visualized by iPSP. The convection of this structure takes about 40 time steps from the time it appears until it finally disappears.

In Fig. 10 the instantaneous intensity fluctuation with equivalent high and low pressure regions on the base is presented for one time step at Mach number 0.7. The position of the *kulite* pressure transducers is blanked in black for clarity. The results on the base show the dynamic behavior of the coherent flow structures in the wake, as well. Moreover, it can be seen that the pressure distribution on the base is organized in a mode-like structure as predicted by numerical flow simulations, [8]. Thus it can be concluded that the predicted pressure pattern is real and not an artifact of the numerical simulation techniques. Further investigations on their distribution (inclination between high and low pressure region), *FFT* response and dependence on boundary layer parameter are on-going and will also be presented in the final publication.

5. Conclusions

Instationary pressure-sensitive paint measurements with sampling-rates of up to 4 kHz were performed for the first time in the *TWM* wind tunnel facility at *UniBwM*. First analysis show a good agreement of the frequency response of the classically acquired pressure signal from the *kulite* pressure transducers and the frequency response derived from the iPSP intensity images. The characteristic vortex dynamics were resolved on the base and on the sting for Mach numbers 0.3 and 0.7. A first look on the intensity fluctuations confirmed the predicted mode-like pressure distribution on the base and visualizes the down-stream convection of large coherent vortices on the sting. The evaluation will be intensified in quantifying and characterizing the mode-structure and further analyzing the convection of the coherent wake structures on the sting.

Acknowledgments

Financial support has been provided by the German Research Foundation (Deutsche Forschungsgemeinschaft – DFG) in the framework of the Sonderforschungsbereich Transregio 40 and the IGSSE (International Graduate School of Science and Engineering) at Technische Universität München.

References

[1] BITTER, M., SCHARNOWSKI, S., HAIN, R. AND KÄHLER, C. J. (2011). High-repetition-rate PIV investigations on a generic rocket model in sub- and supersonic flows. *Exp. Fluids*, **50**, 1019–1030.

[2] LIU, T. AND SULLIVAN, J. (2004). *Pressure and Temperature Sensitive Paints*. Springer Berlin.

[3] BITTER, M. AND KÄHLER, C. J. (2011). Optische Bestimmung von Oberflächen-druck- & Temperaturverteilungen am NACA Profil im Unter- und Transschall. In: *Proceedings of 19. Lasermethoden in der Strömungsmesstechnik*, Ilmenau, Germany.

[4] GREGORY, J., ASAI, K., KAMEDA, M., LIU, T. AND SULLIVAN, J. (2008). A review of pressure-sensitive paint for high-speed and unsteady aerodynamics. *Journ. Aero. Eng.*, **222**, 249–290.

[5] KAMEDA, M., TABEI, T., NAKAKITA, K., SAKAUE, H. AND ASAI, K. (2005). Image measurements of unsteady pressure fluctuation by a pressure-sensitive coating on porous anodized aluminum. *Meas. Sci. Technol.*, **16**, 2517.

[6] ASAI, K., NAKAKITA, K., KAMEDA, M. AND TEDUKA, K. (2001). Recent topics in fast-responding pressure-sensitive paint technology at National Aerospace Laboratory. In: *Proceedings of the 19th International Congress on Instrumentation in Aerospace Simulation Facilities, ICIASF*, Cleveland, USA.

[7] NAKAKITA, K. (2007). Unsteady Pressure Distribution Measurement around 2D-Cylinders Using Pressure-Sensitive Paint. In: *Proceedings of the 26th AIAA Applied Aerodynamics Conference*, Miami, USA.

[8] GÜLHAN, A. (2008). RESPACE - Key technologies for reusable space systems. *Notes on numerical fluid mechanics and multidisciplinary design*, **98**, Springer Berlin.